Nuclear wavepacket motion producing a reversible charge separation in bacterial reaction centers

A.G. Yakovlev[a], A.Y. Shkuropatov[b], V.A. Shuvalov[a,b,*]

[a] *Laboratory of Photobiophysics, Belozersky Institute of Chemical and Physical Biology of Moscow State University, Moscow 119899, Russia*
[b] *Institute of Basic Biological Problems, Russian Academy of Sciences, Pushchino Moscow Region 142292, Russia*

Received 23 November 1999; received in revised form 14 December 1999

Edited by Vladimir Skulachev

Abstract The excitation of bacterial reaction centers (RCs) at 870 nm by 30 fs pulses induces the nuclear wavepacket motions on the potential energy surface of the primary electron donor excited state P*, which lead to the fs oscillations in stimulated emission from P* [M.H. Vos, M.R. Jones, C.N. Hunter, J. Breton, J.-C. Lambry and J.-L. Martin (1994) Biochemistry 33, 6750–6757] and in Q_Y absorption band of the primary electron acceptor, bacteriochlorophyll monomer B_A [A.M. Streltsov, S.I.E. Vulto, A.Y. Shkuropatov, A.J. Hoff, T.J. Aartsma and V.A. Shuvalov (1998) J. Phys. Chem. B 102, 7293–7298] with a set of fundamental frequencies in the range of 10–300 cm^{-1}. We have found that in pheophytin-modified RCs, the fs oscillations with frequency around 130 cm^{-1} observed in the P*-stimulated emission as well as in the B_A absorption band at 800 nm are accompanied by remarkable and reversible formation of the 1020 nm absorption band which is characteristic of the radical anion band of bacteriochlorophyll monomer B_A^-. These results are discussed in terms of a reversible electron transfer between P* and B_A induced by a motion of the wavepacket near the intersection of potential energy surfaces of P* and $P^+B_A^-$, when a maximal value of the Franck–Condon factor is created.

Key words: Reaction center; Electron transfer; Wavepacket; Electron donor; Electron acceptor

1. Introduction

The light energy conversion in bacterial reaction centers (RCs) results in the oxidation of the primary electron donor, bacteriochlorophyll dimer, P, and the reduction of bacteriopheophytin H_A with a ~3 ps time constant at 20°C (see [1,2]). The participation of bacteriochlorophyll monomer B_A (active pigment branch A) in electron transfer (ET) was suggested by ps measurements in 1978 [3] and since that, the mechanism of an involvement of B_A in ET was studied in many further works [4–14]. Recent measurements in pheophytin *a*-reconstituted RCs [6–8,12–14] and in the β-mutant [10] have shown that the free energy level of the $P^+B_A^-$ state in these modified RCs is close to or even below that of P* by 350–550 cm^{-1} [15,16]. The time constant for ET from P* to B_A is about 1.6 ps at 5 K in pheophytin-modified RCs [14], which is similar to that for native RCs. These observations strongly support the model in which B_A is a distinct intermediate in ET from P* to H_A.

In a number of studies, Vos et al.[17–21] have shown that excitation of P by fs laser pulses activates coherent nuclear motions on the P* potential surface, revealed by the oscillatory features in the stimulated emission spectra and kinetics. Similar results were obtained with spontaneous emission measurements [22]. Fourier transforms of the oscillatory part of the kinetics show low-frequency spectra in the range 10–400 cm^{-1} [17–22]. The found modes are very similar to those firstly observed at 31, 73, 110 and 147 cm^{-1} by hole-burning measurements in bacterial RCs in which H_A was prereduced to decrease the ET rate and to improve spectral resolution [23]. The 30 and 140 cm^{-1} modes appear to be strongly coupled to the $P \Rightarrow P^*$ transition [23,24]. Low-frequency modes are also observed in resonance Raman spectra [25–28], and vibrational bands have been reported at 34, 71, 95 and 128 cm^{-1}, which are characteristic of P [26].

Recent works have shown that the fs oscillations in the 800 nm absorption band of B_A can be observed in native as well as B_B-modified RCs of *Rhodobacter sphaeroides* R-26 in the presence of either reduced Q_B or doubly reduced Q_A, and in RCs of the YM210W mutant of the wild-type [29]. When compared with oscillations in stimulated emission, the (30 ± 3) and (12 ± 2) cm^{-1} modes in the 800 nm kinetics were found to be enhanced with respect to the broad structure around 130 cm^{-1} in all types of RCs. The maximal amplitude of both modes was observed in native RCs, while their minimal amplitude is registered in the YM210W mutant in which the rate of ET is significantly decreased [29].

Present work demonstrates that in the pheophytin-modified RCs of *R. sphaeroides* R-26, the fs oscillations in the P*-stimulated emission as well as in the B_A absorption band at 800 nm (see [29]) with a frequency around 130 cm^{-1} are accompanied by the oscillating appearance of the 1020 nm absorption band which is characteristic of the radical anion band of bacteriochlorophyll monomer B_A^- [7,14]. These results are discussed in terms of a reversible ET between P* and B_A induced by a motion of the wavepacket near the intersection of potential energy surfaces of P* and $P^+B_A^-$, when a maximal value of the Franck–Condon factor is created.

2. Materials and methods

RCs of *R. sphaeroides* R-26 were isolated as described in [30], and were pheophytin-modified as described in [6]. The absorption of the

*Corresponding author. Fax: (7)-967-79 05 32.
E-mail: shuvalov@issp.serpukhov.su

Abbreviations: ΔA, light−dark absorbance changes; B_A and H_A, monomeric bacteriochlorophyll and bacteriopheophytin molecules, respectively, located in active branch A; ET, electron transfer; *F*, Franck–Condon factor; P, primary electron donor; Q, quinone; RC, reaction center

PII: S0014-5793(00)01081-4

samples was adjusted to an optical density of 0.5 at 860 nm at 293 K (optical path length of 1 mm). The dithionite (5 mM) was added and the samples were illuminated by non-focused white light of a filament lamp during ~1 min to prereduce the electron acceptor Q_A. All measurements were carried out at room temperature.

The fs spectrometer was based on a home-built cw mode-locked Ti:sapphire laser (26 fs pulse duration, ~200 mW output power, ~100 MHz repetition rate) pumped by cw argon ion laser (Spectra-Physics, USA). After expanding to a ps time scale, the single pulses were extracted by Pockels cell. Then the pulses were amplified in an 8-pass Ti:sapphire amplifier pumped by second harmonic of ns home-built YAG:Nd^{3+} laser. The amplified ps pulses were compressed to its initial fs duration in a pulse compressor. Then the amplified fs pulses were focused in a water cell to produce a continuum. Wavelengths shorter than 850 nm were cut off with a RG 850 filter (Melles Griot). A small fraction (~4%) of the continuum was used as probe and reference pulses, and a main part of the continuum as pump pulses. The pump and probe pulses propagated through delay line and the sample. Then the probe and reference pulses passed through a polychromator connected to OMA (Oriel, France).

The operating frequency of the spectrometer was 1 Hz. Cross-correlation function of the pump and probe pulses showed ~30 fs pulse duration. The relative position of the zero time delay within a 900–1100 nm range was estimated to change by less than 30 fs. The delay between pump and probe pulses was changed with an accuracy of ~20 fs. The probe pulses were depolarized. The difference (light−dark) time-resolved absorbance spectra were a result of averaging of ~50 measurements in the 900–980 range and ~600 measurements in the 980–1060 range. The amplitude of the spectral bands on the broad background was measured at the maximum.

3. Results

Fig. 1 shows the difference (light−dark) absorbance spectra in the range of 900–980 nm (Fig. 1A) and 980–1060 nm (Fig. 1B) for pheophytin-modified RCs from *R. sphaeroides* R-26 at different delays after excitation by ~30 fs pulses at 870 nm. Fig. 2 represents the kinetics of absorbance changes (ΔA) at

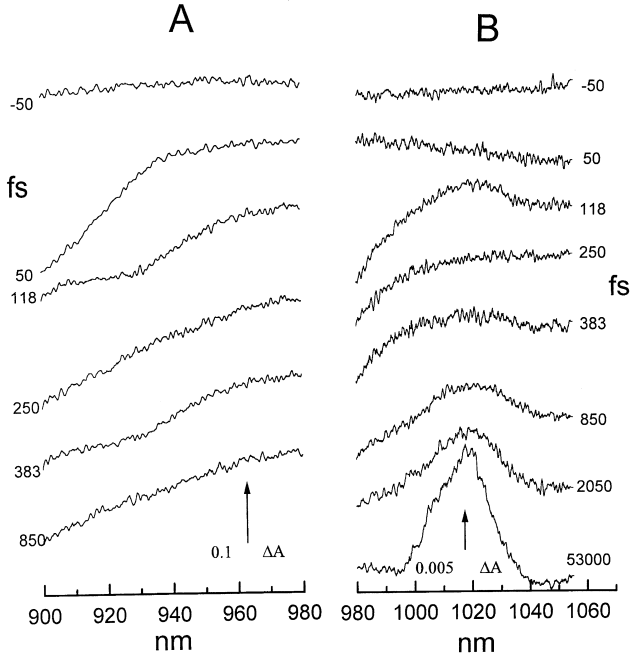

Fig. 1. Difference (light−dark) absorbance spectra measured at various delays at 293 K in pheophytin-modified *R. sphaeroides* R-26 RCs excited by 30 fs pulses at 870 nm. (A) Transient spectra of the stimulated emission from P* in the 900–980 nm range. (B) Spectra of ΔA of the state $P^+B_A^-$ in the 980–1060 nm range. Note the difference of vertical scales for A and B.

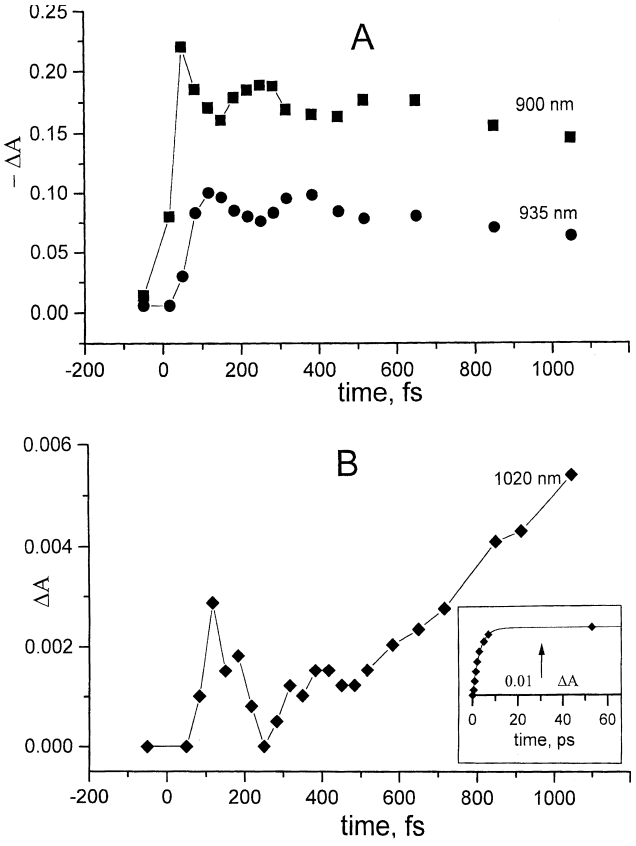

Fig. 2. (A) Kinetics of ΔA at 900 and 935 nm (stimulated emission from P*). (B) Kinetics of ΔA at 1020 nm (center of absorption band of the $P^+B_A^-$ state). A and B kinetics are based on the measured spectra. The inset in B displays the kinetics of ΔA at 1020 nm in ps time scale. The solid curve in the inset shows the exponential growth with a 3 ps rise time.

900 and 935 nm (stimulated emission from P*) (Fig. 2A) and 1020 nm (radical anion band of B_A^-) (Fig. 2B) based on the measured spectra. In agreement with previous measurements [17–21], the stimulated emission from P* has a time dependent position of the maximum. At a 50 fs delay, the stimulated emission displays a peak near 900 nm (895 nm in [20]). During the next ~70 fs, the emission peak shifts to 930 nm (see 118 fs delay) and afterwards shifts back to the blue approaching again the position near 900 nm at 250 fs (Fig. 1A). This behavior of the stimulated emission at the early delays was previously described by the Fourier transform analysis of the kinetics as an oscillation with a fundamental frequency around 130 cm^{-1} [17–21,29].

It was shown [29] that the 130 cm^{-1} oscillation mode which is in phase with that of the long-wavelength stimulated emission is also observed in the kinetics of the bleaching of the 800 nm band characteristic of the B_A ground state absorption. The oscillation of the bleaching around 800 nm was observed in native R-26 RCs [29] as well as in pheophytin-modified RCs (A.M. Streltsov, S.I.E. Vulto, A.Y. Shkuropatov, A.J. Hoff, T.J. Aartsma, V.A. Shuvalov, unpublished results). It was demonstrated that these two kinds of RCs show the same oscillating kinetics at 890 nm and 805 nm and the same Fourier transform spectra. As the bleaching around 800 nm may be attributed to formation of B_A^-, it was suggested that the oscillatory features of the bleaching of the 800 nm band can be related to a reversible formation of the charge-separated

state $P^+B_A^-$ [29]. The measurements of the 1020 nm band reflecting the formation of radical anion B_A^- [7,29,32] are an adequate approach to check this possibility.

Fig. 1 shows that the appearance of the 930 nm emission band of P* at a 118 fs delay is accompanied by the appearance of the 1020 nm absorption band. Note that this delay corresponds also to the maximum of the bleaching at 800 nm [29]. The complete disappearance of the 930 nm band at a 250 fs delay is accompanied by the complete disappearance of the 1020 nm band (Fig. 1A,B) and corresponds to the recovery of the band at 800 nm [29]. Fig. 2B clearly shows that oscillations in absorption at 1020 nm are in phase with the oscillations of stimulated emission of P* ($-\Delta A$) at 930 nm and out of phase with that at 900 nm (Fig. 2A). The first and intense maximum in the kinetics of the 1020 nm band is observed at the 118 fs delay. Then minimum occurs at the 250 fs delay which corresponds to the minimum of the bleaching of the 800 nm band [29], minimum of the stimulated emission at 930 nm and maximum of the stimulated emission at 900 nm. After that, the kinetics of 1020 nm band show again the appearance of a new maximum around 400 fs delay when the kinetics of the 800 nm band shows the next phase of the bleaching [29]. It is interesting to note that the second maximum is smaller in amplitude than the first one in the kinetics of the bleaching at 800 nm [29] as well as in the kinetics of the appearance of the 1020 nm band. After $\sim$500 fs delay, the 3 ps exponential growth of the irreversible ET is observed which is accompanied by the gradual increasing of the absorption band at 1020 nm (Fig. 2B and inset for ps delays) reflecting the irreversible formation of $P^+B_A^-$ (see also [14]).

4. Discussion

Thus the oscillating part of the kinetics of the 1020 nm band ($+\Delta A$) is a mirror image of that of the kinetics of the appearance ($-\Delta A$) of the 930 nm emission from P* (Figs. 1 and 2) as well as of the kinetics of the bleaching at 800 nm [29]. This indicates that the shift of the P* emission to the longest wavelength is accompanied by the reversible formation of the state $P^+B_A^-$ since the appearance of the 1020 nm band is characteristic of the radical anion band of the bacteriochlorophyll monomer [7,14,31]. The ratio of amplitudes of the 1020 nm band at 118 fs delay and 53 ps delay (Fig. 1B) is about 1:6.7, respectively. According to the exponential growth of the $P^+B_A^-$ state with about 3 ps rise time at room temperature (Fig. 2B, inset), this ratio should be 1:30. These facts show that the reversible appearance of the $P^+B_A^-$ state at 120 fs delay is rather due to the coherent effect connected to the nuclear wavepacket motion. The reversible adiabatic ET between P* and B_A seems to take place when the nuclear wavepacket moves on the potential energy surface of the state P*. Only after $\sim$500 fs delay, the gradual increase of the absorption band at 1020 nm reflecting the irreversible formation of $P^+B_A^-$ is observed (Fig. 2B).

The data presented here can be explained by an energy level scheme (Fig. 3) which shows the potential energy curves for the PB, P*B, $P^+B_A^-$ and $P^+(B_A^-)$* states representing cross-sections of the potential energy surfaces. The wavepacket is firstly formed on the potential energy surface of P* due to the excitation of P by 30 fs pulse. Since this pulse is spectrally very broad ($\sim$900 cm^{-1}), many vibrational levels are involved in the superposition of their wavefunctions creating the wavepacket [32]. This wavepacket is like a semiclassical particle which starts moving on the potential surface of P*. Since the appearing of the bleaching at 800 nm [29] and of the absorption band at 1020 nm (Fig. 1B) at $\sim$120 fs delay corresponds to the appearance of the long-wavelength ($\sim$930 nm) stimulated emission from P* (Fig. 1A), the intersection of the potential energy curves of P* and $P^+B_A^-$ is close to the long-wavelength side of the stimulated emission from P* (see Fig. 3). When the wavepacket approaches the intersection point, the maximal value of the Franck–Condon factor necessary for the electron exchange between P* and B_A is created. Under these conditions, the exchange interaction time (τ) can be expressed by a product of two factors including an exchange interaction energy (V) and the Franck–Condon factor (F) (found as an overlap integral between the P* and $P^+B_A^-$ wavepackets):

$$1/\tau = (2V/\pi\hbar)F \quad (1)$$

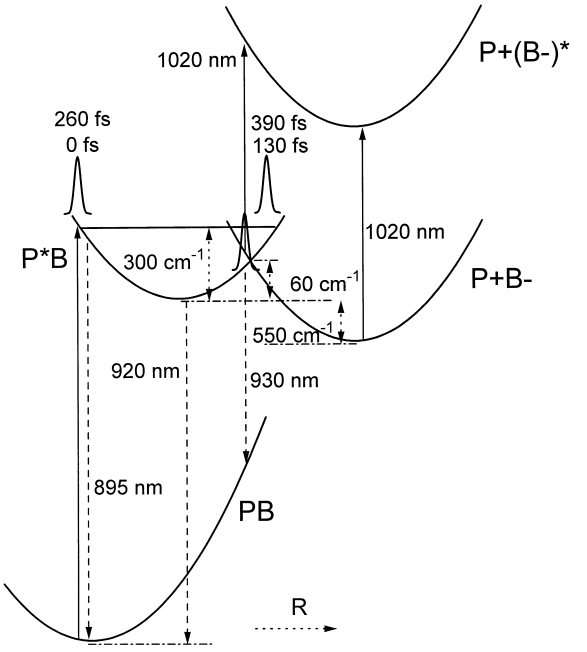

Fig. 3. Tentative energy level scheme for states PB, P*B, P^+B^-, $P^+(B_A^-)$*. The potential energy curves for these states are shown as one-dimensional cross-section of the corresponding potential energy surfaces. The wavepacket is created by 30 fs pulses at 870 nm on the P*B potential energy surface for the 130 cm^{-1} mode. See text for other details.

For further discussion, let us suggest that the displacement of the $P^+(B_A^-)$* surface is not remarkable with respect to $P^+B_A^-$, so the shape of the absorption band at 1020 nm is mostly independent of the position of the wavepacket on the $P^+B_A^-$ potential surface. The activationless ET from P* [29] shows that the energy corresponding to the intersection of the P* and $P^+B_A^-$ potential surfaces is close to the bottom of the P* surface. If the energy of the wavepacket is larger than that of the intersection, a momentum of the wavepacket is larger than zero at the intersection. In spite of that the absorption amplitude at 1020 nm approaches probably the maximum at the intersection (118 fs delay, Fig. 2B). When the wavepacket approaches the potential energy maximum (150 fs delay) and moves back toward to the short-wavelength

emission, it approaches again the intersection (183 fs delay). The absorption at 1020 nm is maximal again, but weaker than at first approach probably due to a dephasing of a coherence. The minimum of the absorption at 1020 nm is observed at 250 fs delay when the wavepacket approaches the short-wavelength emission. This shows that the intersection is closer to the long-wavelength emission side and its energy is slightly above the bottom of the potential surface. Using the wavepacket motion time, one can estimate that this energy is ~ 60 cm^{-1} (Fig. 3). Then the same process is repeated with weaker amplitudes due to the dephasing process. After ~ 500 fs delay, the exponential growth of the band at 1020 nm is observed due to the irreversible ET.

The reasons for a small probability of the irreversible ET at ~ 120 fs delay can be considered. One of those can be related to a relatively large half-width of the wavepacket (~ 900 cm^{-1}) and small slit between two surfaces induced by the exchange interaction (energy V) between P* and $P^+B_A^-$ (average value of 15 cm^{-1}, see [33,34]). Due to this large difference, only a small probability exists for the wavepacket to be irreversibly transferred on the $P^+B_A^-$ surface. As a result, the reversible ET between P* and B_A is only observed when the wavepacket is near the intersection at 120 fs. On the other hand, the ratio of the exchange interaction time (see Eq. 1) between P* and B_A ($\pi\hbar/2V$) corresponds to 600 fs and a half-width of the oscillating maximum at 1020 nm around 120 fs delay (~ 100 fs, see Fig. 2) is about six. This means that only 1:6 of electron density can be shifted from P* to B_A within 100 fs. This value corresponds to the ratio (1:6.7) of the 1020 nm band amplitudes measured at 118 fs and 53 ps, respectively. It shows that the Franck–Condon factor for ET at 118 fs delay is probably close to one and the 1020 nm band amplitude is limited by the exchange interaction time at this early delay (see Eq. 1). The irreversible ET is probably connected to the lower frequency modes which form their potential energy surfaces having the intersection with the $P^+B_A^-$ surface. The study of this ET is in progress.

Acknowledgements: We thank Dr. A.V. Sharkov for help in construction of fs spectrometer and V.A. Shkuropatova for preparing the samples. Support by the Russian Fundamental Research Foundation (Grant N 99-04-49120), 'Universities of Russia - Fundamental Researches' and NWO (The Netherlands) grants is gratefully acknowledged.

References

[1] Shuvalov, V.A. (1990) Primary Light Energy Conversion at Photosynthesis, Nauka (in Russian), Moscow.
[2] Hoff, A.J. and Deisenhofer, J. (1997) Phys. Rep. 287, 1–35.
[3] Shuvalov, V.A., Klevanik, A.V., Sharkov, A.V., Matveetz, Y.A. and Krukov, P.G. (1978) FEBS Lett. 91, 135–139.
[4] Shuvalov, V.A. and Duysens, L.N.M. (1986) Proc. Natl. Acad. Sci. USA 83, 1690–1694.
[5] Chekalin, S.N., Matveetz, Y.A., Shkuropatov, A.Y., Shuvalov, V.A. and Yartzev, A. (1987) FEBS Lett. 216, 245–248.
[6] Shkuropatov, A.Y. and Shuvalov, V.A. (1993) FEBS Lett. 322, 168–171.
[7] Arlt, T., Schmidt, S., Lauterwasser, C., Meyer, M., Scheer, H. and Zinth, W. (1993) Proc. Natl. Acad. Sci. USA 90, 11757–11761.
[8] Schmidt, S., Arlt, T., Hamm, P., Huber, H., Nagele, T., Wachtveitl, J., Meyer, M., Scheer, H. and Zinth, W. (1994) Chem. Phys. Lett. 223, 116–120.
[9] Bixon, M., Jortner, J., Michel-Beyerly and M.E. (1992) in: The Photosynthetic Bacterial Reaction Center II (Breton, J. and Vermeglio, A., Eds), pp. 291–300, Plenum Press, New York.
[10] Kirmaier, C., Laporte, L., Schenck, C.C. and Holten, D. (1995) J. Phys. Chem. 99, 8910–8917.
[11] Chan, C.-K., DiMagno, T.J., Chen, L.X.-Q., Norris, J.R. and Fleming, G.R. (1991) Proc. Natl. Acad. Sci. USA 88, 11202–11206.
[12] Franken, E.M., Shkuropatov, A.Y., Francke, C., Neerken, S., Gast, P., Shuvalov, V.A., Hoff, A.J. and Aartsma, T.J. (1997) Biochim. Biophys. Acta 1319, 242–250.
[13] Franken, E.M., Shkuropatov, A.Y., Francke, C., Neerken, S., Gast, P., Shuvalov, V.A., Hoff, A.J. and Aartsma, T.J. (1997) Biochim. Biophys. Acta 1321, 1–9.
[14] Kennis, J.T.M., Shkuropatov, A.Y., Van Stokkum, I.H.M., Gast, P., Hoff, A.J., Shuvalov, V.A. and Aartsma, T.J. (1997) Biochemistry 36, 16231–16238.
[15] Shuvalov, V.A. and Yakovlev, A.G. (1998) Membr. Cell Biol. 12, 563–569.
[16] Nowak, F.R., Kennis, J.T.M., Franken, E.M., Shkuropatov, A.Y., Yakovlev, A.G., Gast, P., Hoff, A.J., Aartsma, T.J. and Shuvalov, V.A. (1998) Proceedings of the XI Int. Congr. on Photosynthesis, Budapest, Hungary, pp. 783–786, Kluwer, Acad. Publs., Dordrecht.
[17] Vos, M.H., Jones, M.R., Breton, J., Lambry, J.-C. and Martin, J.-L. (1996) Biochemistry 35, 2687–2692.
[18] Vos, M.H., Rappaport, F., Lambry, J.-C., Breton, J. and Martin, J.-L. (1993) Nature 363, 320–325.
[19] Vos, M.H., Jones, M.R., McGlynn, P., Hunter, C.N., Breton, J. and Martin, J.-L. (1994) Biochim. Biophys. Acta 1186, 117–122.
[20] Vos, M.H., Jones, M.R., Hunter, C.N., Breton, L., Lambry, J.-C. and Martin, J.-L. (1994) Biochemistry 33, 6750–6757.
[21] Vos, M.H., Jones, M.R., Hunter, C.N., Breton, L. and Martin, J.-L. (1994) Proc. Natl. Acad. Sci. USA 91, 12701–12705.
[22] Stanley, R.J. and Boxer, S.G. (1995) J. Phys. Chem. 99, 859–863.
[23] Shuvalov, V.A., Klevanik, A.V., Ganago, A.O., Shkuropatov, A.Y. and Gubanov, V.S. (1988) FEBS Lett. 237, 57–60.
[24] Lyle, P.A., Kolaczkowsky, S.V. and Small, G.J. (1993) J. Phys. Chem. 97, 6924–6933.
[25] Shreve, A.P., Cherepy, N.J., Franzen, S., Boxer, S.G. and Mathies, R.A. (1991) Proc. Natl. Acad. Sci. USA 88, 11207–11211.
[26] Cherepy, N.J., Shreve, A.P., Moore, L.J., Franzen, S., Boxer, S.G. and Mathies, R.A. (1994) J. Phys. Chem. 98, 6023–6029.
[27] Donohoe, R.J., Dyer, R.B., Swanson, B.I., Violette, C.A., Frank, H.A. and Bocian, D.F. (1990) J. Am. Chem. Soc. 112, 6716–6723.
[28] Palaniappan, V., Aldema, M.A., Frank, H.A. and Bocian, D.F. (1992) Biochemistry 31, 11050–11058.
[29] Streltsov, A.M., Vulto, S.I.E., Shkuropatov, A.Y., Hoff, A.J., Aartsma, T.J. and Shuvalov, V.A. (1998) J. Phys. Chem. B 102, 7293–7298.
[30] Shuvalov, V.A., Shkuropatov, A.Y., Kulakova, S.M., Ismailov, M.A. and Shkuropatova, V.A. (1986) Biochim. Biophys. Acta 849, 337–348.
[31] Fajer, J., Bruno, D.C., Davis, S., Forman, A. and Spaulding, L.D. (1975) Proc. Natl. Acad. Sci. USA 72, 4956–4960.
[32] Sokolov, A.A., Loskutov, Y.M. and Ternov, I.M. (1962) Quantum Mechanics, State Education Publisher, Moscow (in Russian).
[33] Parson, W., Warshel, A., Creighton, S. and Norris, J. (1988) in: The Photosynthetic Bacterial Reaction Center (Breton, J. and Vermeglio, A., Eds.), pp. 309–317, Plenum Press, New York.
[34] Marcus, R.A. (1988) in: The Photosynthetic Bacterial Reaction Center (Breton, J. and Vermeglio, A., Eds.), pp. 389–398, Plenum Press, New York.